frontiers | Frontiers in Earth Science

TYPE Original Research
PUBLISHED 09 January 2023
DOI 10.3389/feart.2022.1036902

OPEN ACCESS

EDITED BY
Dun Wu,
Anhui Jianzhu University, China

REVIEWED BY
Dawei Lv,
Shandong University of Science and Technology, China
Jian Chen,
Anhui University of Science and Technology, China
Yuzhuang Sun,
Hebei University of Engineering, China

*CORRESPONDENCE
Liugen Zheng,
lgzheng@ustc.edu.cn

SPECIALTY SECTION
This article was submitted to Geochemistry, a section of the journal Frontiers in Earth Science

RECEIVED 05 September 2022
ACCEPTED 22 September 2022
PUBLISHED 09 January 2023

CITATION
Zheng L, Zhang L, Wang Y, Chen Y, Chen Y, An S and Xu Y (2023), Content and distribution of mercury in coal and its relation to depositional environment—A case study on coals from the Shanxi Formation in Huainan Coalfield.
Front. Earth Sci. 10:1036902.
doi: 10.3389/feart.2022.1036902

Content and distribution of mercury in coal and its relation to depositional environment—A case study on coals from the Shanxi Formation in Huainan Coalfield

Liugen Zheng[1,2]*, Liqun Zhang[1,2], Yunlong Wang[1,2], Yeyu Chen[1,2], Yongchun Chen[3], Shikai An[3] and Yanfei Xu[3]

[1]School of Resources and Environmental Engineering, Anhui University, Hefei, China, [2]Anhui Province Engineering Laboratory for Mine Ecological Remediation, Hefei, Anhui, China, [3]National Engineering Laboratory of Coal Mine Ecological Environment Protection, Huainan, Anhui, China

Mercury in coals might emit into the environment from coal combination, and finally cause environmental pollution. In this paper, 26 coal samples were selected from No. 1 which is coal in the Shanxi Formation of Zhangji and Xinjier mines in the Huainan coalfield. The mineralogical and geochemical components of coal samples were determined by DMA-80 mercury-measuring instrument, XRF, XRD, ICP-MS, and the relationship between the depositional environment of the coal seam and mercury enrichment was analyzed. The results show that the mercury content of coal in the study area ranged from 0.03 to 0.93 μg/g, with an arithmetic means of 0.21 μg/g, higher than the background values of coal in China and the world. The mercury content of Shanxi Formation coal varied among different mines, the arithmetic mean value of mercury in Zhangji coal mine and Xinjier mine coal is 0.35 μg/g and 0.12 μg/g respectively. Due to the complex depositional environment and depositional facies, the distribution of mercury content in the coal seam is quite different. XRD, Microscopic observation and the ratio of (CaO + MgO + Fe_2O_3)/(SiO_2+ Al_2O_3) and Al_2O_3/TiO_2 show that the main mineral in the depositional environment of this study area is kaolinite, quartz and pyrite, and the depositional facies are intercontinental and sea-land, so the parent rock type belongs to acid bedrock. The Ni/Co, Sr/Ba, and Sr/Cu ratios were used to indicate a weak oxidation-reduction, Marine salt water, and an arid and hot environment. The vertical distribution of mercury in coal and the characteristics of the depositional environment are combined to show that mercury in coal is easily affected by redox conditions, paleosalinity and paleoclimate in the depositional environment. At the same time, mercury accumulation is more easily in the depositional environment dominated by seawater intrusion than in the terrigenous input.

KEYWORDS

coal, mercury, depositional environment, representation, form

1 Introduction

China is the world's largest coal producer and consumer and also accounts for nearly 30% of global energy-related CO_2 emissions due to its heavy reliance on coal (Chen et al., 2022). Mercury is a highly toxic element that exists in the organic and inorganic components of coal. Due to its characteristics of remote migration and strong redox capacity, it is prone to migration, transformation and redistribution during coal processing and utilization, thus affecting the environment and human health (Lv et al., 2019; Luo et al., 2013; Chen et al., 2014a; Zhao et al., 2019). Mercury in coal is usually converted into Hg^0 and $HgCl_2$ in the process of coal burning and enters the atmosphere in the form of steam, thus causing global pollution (Yang et al., 2020; Cheng et al., 2017). According to global statistics of mercury release, the global mercury release is 2,220 t, and coal burning accounts for 21% in 2018 (United Nations Environment Programme, 2019). Coal burning has been recognized as the world's leading source of man-made mercury emissions (Tian et al., 2014; Chen et al., 2016; Hu and Cheng, 2016; Guo et al., 2018).

The distribution of mercury content in coal is obviously different with different regions and coal-accumulating periods. The average mercury content of coal in China is 0.19 μg/g (Zheng et al., 2007a), slightly higher than the average mercury content in coal in the United States (0.17 μg/g) and the world (0.1 μg/g) (Finkelman, 1993). In general, the distribution of mercury content in Chinese coal shows a trend of low abundance in northwest, north and central regions, meanwhile, with high abundance in northeast and southwest regions. The mercury content in middle Devonian coal ranged from 0.08 to 0.23 μg/g, with an average of 0.17 μg/g (Dai et al., 2006), and that in late Triassic coal ranged from 0.34 to 10.5 μg/g, with an average of 1.61 μg/g (Zhang et al., 1999). Zheng statistical table of mercury content in coal of different coal-accumulating stages in China showed that middle Jurassic = Paleogene and Neogene < Early Jurassic < Early Permian < Middle Devonian < Carboniferous-Early Permian < Late Permian < Late Triassic (Zheng et al., 2007b). The distribution of mercury in different coal-accumulating periods is different, which is mainly caused by the different depositional environments in the coal-forming period. Some trace elements were more easily enriched in the depositional environment with strong oxidation (Chen et al., 2021; Zhang L. Q. et al., 2022). The results of research on mercury in the coal of Zhuji mining area of Huainan coalfield show that mercury is more likely to accumulate in the freshwater environment than in saltwater environment (Wang G. et al., 2018). Therefore, the causes of mercury enrichment in coal are very complex due to the length of coal generation time and the great difference in coal generation environment, and extensive and in-depth research is still needed.

Huainan coalfield is one of China's 14 billion tons of coal production base and six coal power bases. With the massive mining of coal resources, it has entered the deep mining stage of Shanxi

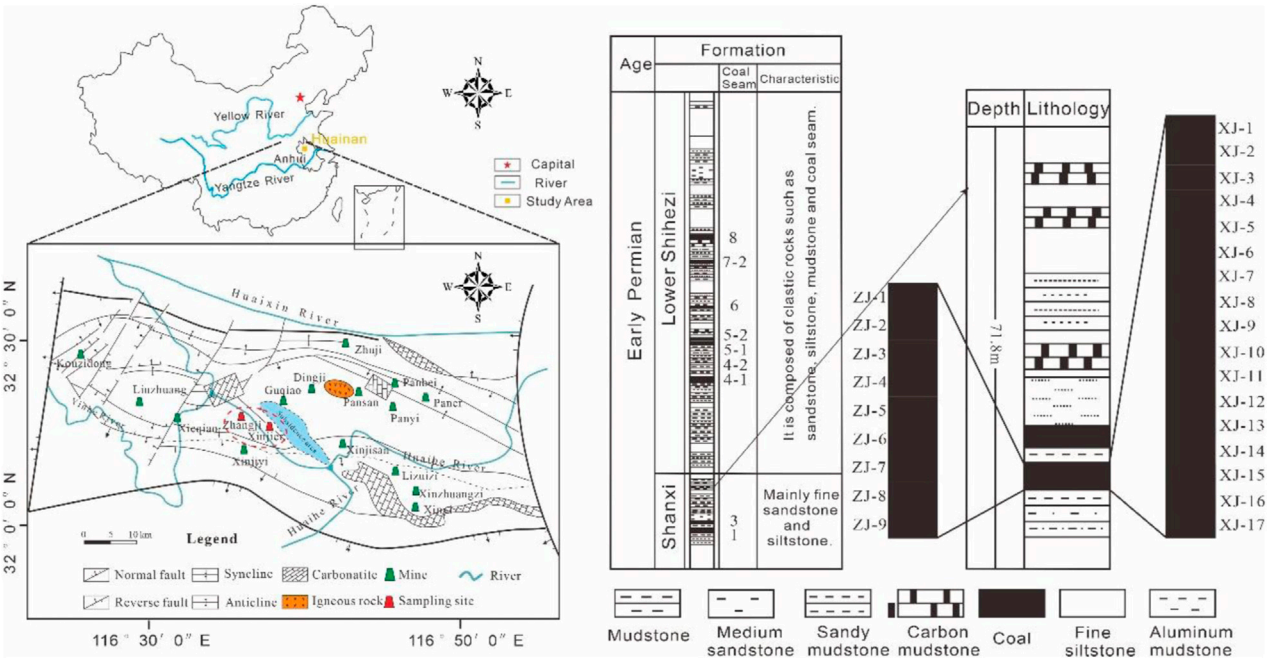

FIGURE 1
Geological stratigraphic map of Huainan coalfield.

TABLE 1 Ash composition ratio of coal.

Sample	Al_2O_3	SiO_2	CaO	Fe_2O_3	MgO	P_2O_5	Na_2O	TiO_2	C	S/A	A/T
ZJ-1	1.54	2.09	0.02	5.22	0.86	0.01	0.05	0.05	1.68	1.36	30.80
ZJ-2	3.00	5.50	0.01	1.01	0.31	0.02	0.05	0.38	0.16	1.83	7.89
ZJ-3	2.18	1.41	0.04	1.33	0.13	0.01	0.05	0.09	0.42	0.65	24.22
ZJ-4	2.89	0.31	0.19	1.26	0.03	0.01	0.05	0.04	0.46	0.11	72.25
ZJ-5	2.94	2.37	0.67	1.88	0.09	0.04	0.05	0.11	0.50	0.81	26.73
ZJ-6	1.81	2.02	0.88	1.05	0.26	0.03	0.06	0.08	0.57	1.12	22.63
ZJ-7	5.98	4.40	0.76	1.27	0.23	0.08	0.06	0.34	0.22	0.74	17.59
ZJ-8	6.21	3.98	0.24	1.02	0.14	0.03	0.06	0.51	0.14	0.64	12.18
ZJ-9	5.32	3.80	0.35	3.08	0.07	0.02	0.06	0.36	0.38	0.71	14.78
XJ-1	3.21	3.27	1.01	1.62	0.05	0.02	0.01	0.11	0.41	1.02	29.18
XJ-2	7.84	7.73	0.67	0.89	0.06	0.05	0.06	0.18	0.10	0.99	43.56
XJ-3	4.09	4.41	0.63	2.61	0.03	0.03	0.03	0.21	0.38	1.08	19.48
XJ-4	7.32	10.22	0.89	1.56	0.13	0.12	0.13	0.34	0.15	1.40	21.53
XJ-5	5.7	6.25	0.71	0.45	0.07	0.07	0.05	0.16	0.10	1.10	35.63
XJ-6	8.33	8.21	0.66	0.84	0.15	0.15	0.08	0.23	0.10	0.99	36.22
XJ-7	2.69	2.65	0.58	0.53	0.23	0.2	0.02	0.14	0.25	0.99	19.21
XJ-8	9.94	22.63	3.21	0.91	0.85	0.07	0.17	0.41	0.15	2.28	24.24
XJ-9	10.65	24.13	4.98	1.71	1.26	0.04	0.11	0.48	0.23	2.27	22.19
XJ-10	7.46	15.06	2.95	1.22	0.34	0.13	0.09	0.17	0.18	2.02	43.88
XJ-11	5.67	7.33	1.79	0.54	0.15	0.02	0.04	0.41	0.19	1.29	14.92
XJ-12	7.26	8.47	0.31	1.78	0.17	0.23	0.05	0.51	0.20	1.17	14.24
XJ-13	2.05	2.13	0.79	0.52	0.06	0.2	0.01	0.11	0.33	1.04	18.64
XJ-14	4.61	3.53	0.44	0.72	0.21	0.03	0.07	0.37	0.17	0.77	12.46
XJ-15	1.48	2.26	0.32	0.4	0.13	0.02	0.04	0.11	0.23	1.53	13.45
XJ-16	1.59	5.11	0.71	0.49	0.23	0.17	0.11	0.15	0.17	3.21	10.60
XJ-17	2.47	3.27	0.89	0.57	0.18	0.03	0.05	0.18	0.29	1.32	13.72

Note: C=[w(CaO)+w(MgO)+w(Fe_2O_3)]/[w(SiO_2)+w(Al_2O_3)]; A/S: SiO_2/Al_2O_3; A/T: Al_2O_3/TiO_2.

Formation 1 coal seam. The coal seam of deep Shanxi Formation is the main coal seam in the later period of Huainan coalfield, which is a lump of important and special coal accumulating period. The coal-bearing formation of the Shanxi Formation in the early Permian was distributed in the foreland fold and thrust belt of the Dabie-Sulu orogenic belt and its front area. In the early stage of mineralization and post-diagenesis, which has experienced many times of strong regional geological tectonic movements, and of which the depositional environment and facies are very complex and special (Zhang et al., 2020). In this paper, the mercury content of coal in the Huainan Shanxi Formation was analyzed by means of mineral content determination and depositional environmental characteristics, so as to understand the origin of its enrichment. The study on the content and distribution characteristics of mercury in Huainan Shanxi Formation combined with depositional environmental characteristics is not only of great significance to correctly control and evaluate the release and environmental effect of mercury in coal utilization in China but also can enrich the related research on mercury in coal in North China.

2 Geologic setting

Huainan coalfield is located in the south of north China coal accumulation area, in the north central Anhui province, with Huainan city as the major structure, extending into Chuxian area in the east and extending around Fuyang in the west. The plane is long ellipse in the northwest direction, about 100 km long, 20–30 km wide and an area of 2,500 km^2, and which has an average annual coal production of nearly 8×10^7 t. The Carboniferous-Permian period was an important peat-forming period in the Huainan Coalfield (Wei et al., 2021). The coal-bearing strata in this area include the Benxi Formation of the Late Carboniferous, the Upper Shihezi Formation, Lower Shihezi Formation, Taiyuan Formation, Shanxi Formation of the Early Permian. The thickness of the Upper Shihezi Faomation is between 600 and 800 m, the lithology is continental sandstone, mudstone and limestone, and whcih includes 13 and 11 coal seams. The Lower Shihezi Formation has a thickness of 100–150 m and is lithologically composed of mudstone, sandstone and siltstone. The coal seams contain

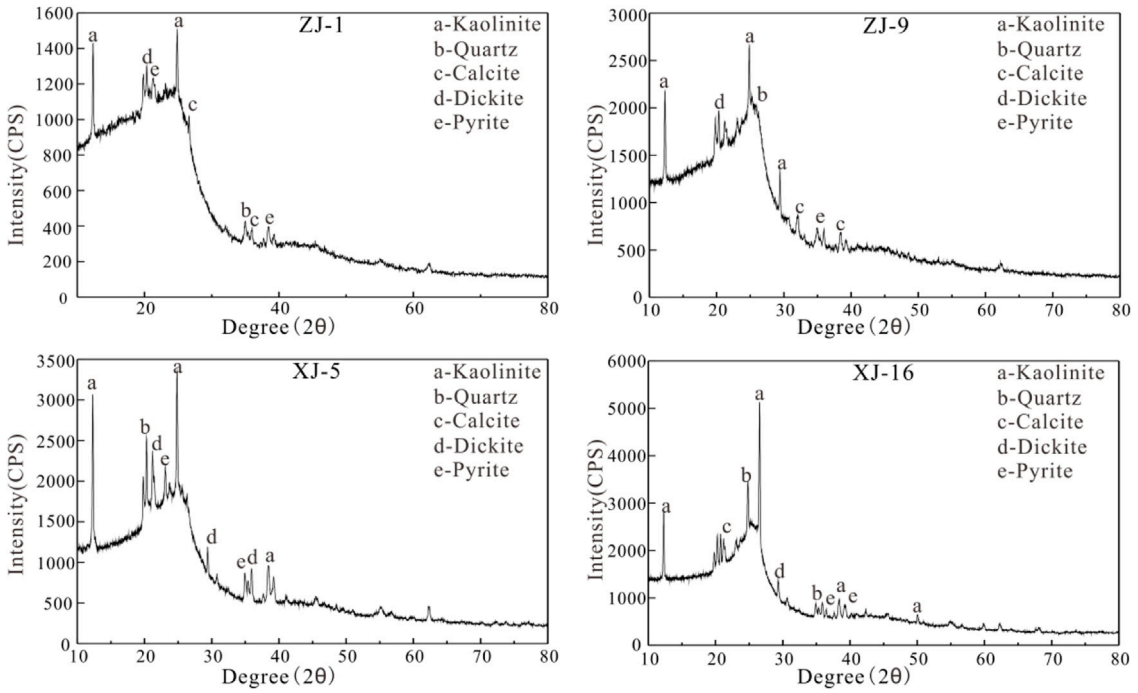

FIGURE 2
X-ray diffraction spectrum of coals in the Shanxi Formation.

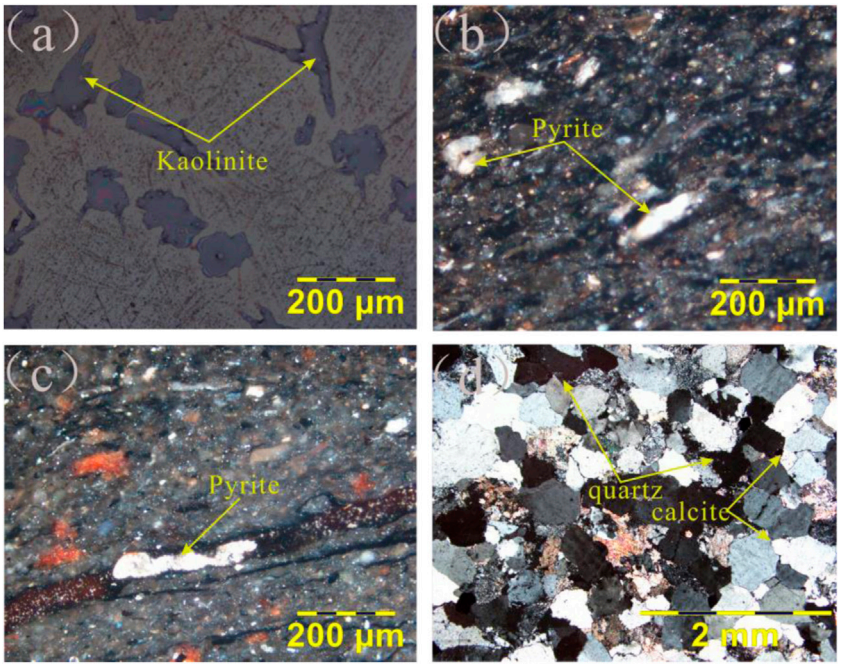

FIGURE 3
Mineral composition of coals in the Shanxi Formation under light microscope. (The labels indicate the names of the minerals contained, **(A)** Kaolinite, **(B)** Pyrite, **(C)** Pyrite, **(D)** quartz and calcite).

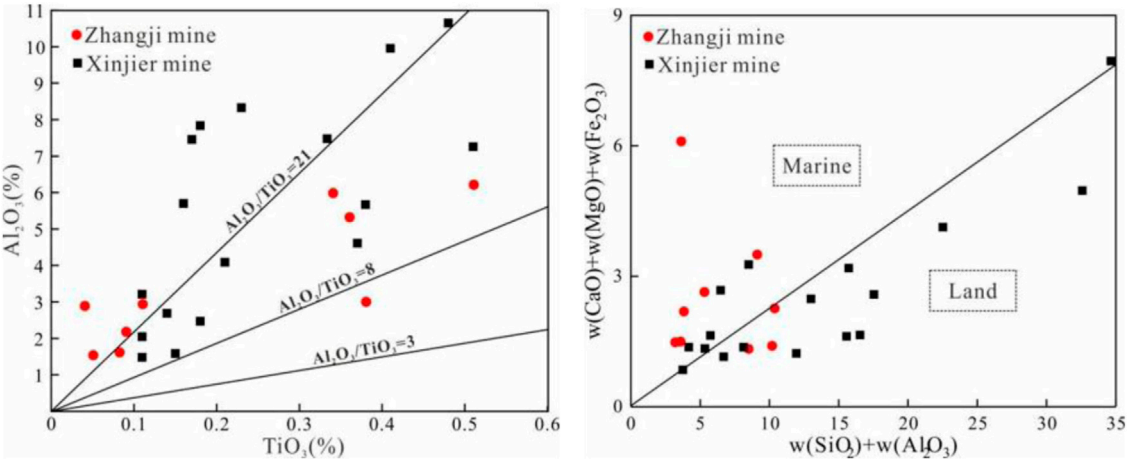

FIGURE 4
Lithological parameters and sedimentary environment ratio.

TABLE 2 The average mercury concentration of Huainan Coalfield Shanxi Formation and other country/region coals (μg/g).

Region	Zhangji mine	Xinjier mine	Huaibei[a]	North China[b]	Yunnan[c]	Guizhou[c]	China[d]	America[e]	World[f]	crust[g]
Range	0.11–0.78	0.03–0.93	0.06–0.79	0.1–0.5	0.03–0.73	0.10–2.67	0–45.0	0–10.0	0.02–1.0	—
Samples	9	17	26	252	34	88	1,699	0.17	—	2,246
concentration (μg/g)	0.35	0.12	0.263	0.20	0.19	0.172	0.19	0.17	0.1	0.08

[a]From Zheng et al. (2007).
[b]From Huang et al. (2002).
[c]From Li et al. (2006).
[d]From Zheng et al. (2007).
[e]From Finkelman (1994).
[f]From Dai et al. (2003).
[g]From Li (1994).

9–2, 8, 7, 6, 5, and 4. The total thickness of Shanxi Formation is 60–70 m. The main lithology of Taiyuan formation is stratified limestone, mudstone and sandstone, which contains a total of seven thin coal beds. Due to the poor coal quality, many of them are unrecoverable (Figure 1).

Zhangji Coal Mine is located in the north wing of The Xieqiao syncline, at the southeast dip end of the Chenqiao anticline. The overall shape is a fan-shaped monocline structure with an incomplete arc turning trend. It covers an area of about 71 km^2 and has a coal reserve of 1.8×10^9 t. Xinjier Coal Mine is located in the south wing of Xieqiao syncline. A series of thrust faults extending from east to west are developed in this area, forming a thrust nappe structural system with Fufeng thrust fault as the main body and it covers an area of about 30km^2, and which has a coal reserve of 4.15×10^8 t (Figure 1).

3 Sampling and determination

During the exploration of the Zhangji and Xinjier mine, according to the standard of GB/T 482-2008 Coal Seam Sampling method, a total 26 samples were collected from Shanxi Formation. Among them, nine samples were collected by Zhangji Mine, and the sampling point interval was 0.5 m, respectively marked as ZJ-1~ZJ-9. 17 samples were collected from Xinjier Mine, with sampling points spaced at 0.3 m apart, respectively marked as XJ-1~XJ-17. To avoid weathering and contamination of coal samples, the collected samples were promptly stored and sealed in plastic bags for later use.

The Hg content was determined by mercury-measuring instrument (DMA-80, milestone, Italy). Parameters were set as follows: drying temperature 300°C, drying time 80 s, decomposition temperature 900°C, decomposition time 180 s,

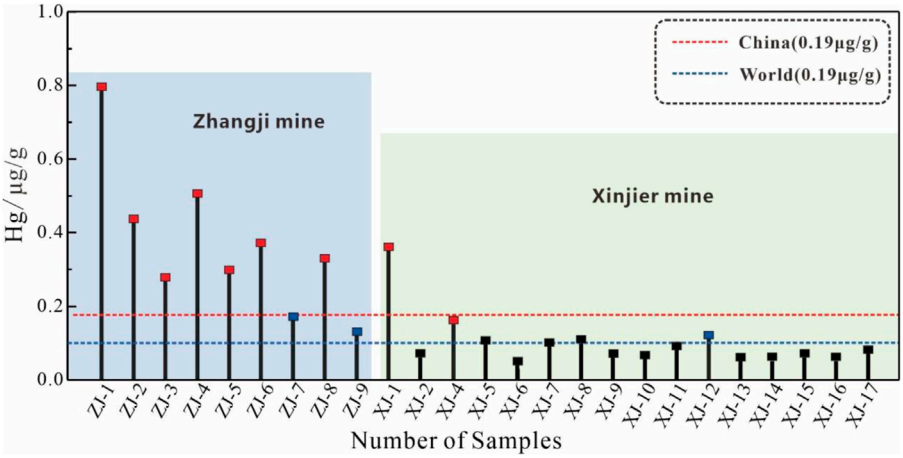

FIGURE 5
Mercury content distribution in coal of Huainan Shanxi Formation.

waiting time 80 s, amalgamation time 12 s, recording measurement signal time 30 s, oxygen pressure 4×10^5 Pa.

The constant element oxide (Al_2O_3, SiO_2, CaO, Fe_2O_3, MgO, P_2O_5, Na_2O, and TiO_2) after 815°C ashing completely using (ZSX Primus II type, Rigaku Industrial Corporation, Japan), parameters setting, electric refrigeration Si-PIN 6 was the sensitive area of the detector for X 6 $mm^2\times0.5$ mm, the test voltage for 17 kV, current for 7 mu A. The mineral composition was determined by XRD (SmartLab 9, Rigaku Industrial Corporation, Japan). Parameters were set: test voltage 40 kV, test current 40 mA, scanning speed 3°/min, step length 0.020°, Angle test 0°–90°.

A coal sample of 1 g was weighed and placed in a Teflon crucible, and then 13 ml of wang Hydrated water (HNO_3:HF:HClO=5:5:3) was added for decomposition. After standing for 12 h at room temperature, it was heated on an electric heating plate at 150°C. Acid was added continuously until the solution became colorless and transparent. Nine trace elements (including B, Co, Ni, Cu, U, Sr, Ba, Mo, and Ga) were determined by ICP-MS (Agilent 7500cx, Agilent, United States). Parameter setting: power 1500 W, carrier gas (Ar) flow 0.95 L/min, atomization gas (Ar) flow 0.25 L/min, scanning number 30 times.

4 Results and discussion

4.1 Minerals and major element oxides

The ash composition of coal can not only predict the mineral types in coal, but also predict the parent rock properties and judge the depositional environment characteristics (Eskenazy et al., 2010; Harrar et al., 2022). As Table 1 shows, the chemical composition of coal ash consist mainly of SiO_2 and Al_2O_3. Lesser proportions of Fe_2O_3, CaO and minor amounts of MgO, TiO and other oxides in study area. The ash pertains to the SiO_2-Al_2O_3-Fe_2O_3-CaO type, indicating that more terrestrial minerals were transported to the study area and deposited on the coastal deltaic plain with large amounts of clastics (Qin et al., 2018; Zhang Q. et al., 2022).

The main minerals in the study coal samples were identified by XRD and microscopic observation. (Figures 2, 3). Clay minerals were the major minerals, followed by carbonate minerals and sulfide minerals. Quartz is mainly in the shape of a random group in The Shanxi Formation, which is filled between other mineral crystals (Figure 3D); Additionally, the clay mineral is filled in the cell cavity of the organic microscopic component (Figure 3A); the pyrite is tuberculous or filled with fissures or in the form of small spheres (Figures 3B,C). The calcite is granular in rock samples (Figure 3D). The concentrations of clay minerals in the Xinjier Mine were relatively higher than in the Zhangji Mine, which also suggests more terrigenous inputs occurred in The Shanxi Formation of Xinjier Mine.

The Al_2O_3/TiO_2 ratio is a geodetic parameter used to judge the source lithology of the source area. Its value ranges from 3 to 8, indicating the basic rock. 8–21 is neutral rock; and greater than 21 is acid rock (Dai et al., 2013; Chen et al., 2014b; Li C. H. et al., 2018). The Al_2O_3/TiO_2 values in the Shanxi Formation range from 8 to 66, most of which are varied from 21 to 70, with an average of 23, indicating that the study area was mainly felsic depositional rocks (Figure 4).

The ratio $(CaO+MgO+Fe_2O_3)/(SiO_2+Al_2O_3)$ (the value of C) of coal can be used as the depositional environment index of peat accumulation stage (Chou, 2012; Dai et al., 2012). The value of C ranges from 0.03 to 0.22, the coal seams formed in continental marsh environment, not affected by the seawater. The value of C ranges from 0.23 to 1.23, coal seam formed in the

TABLE 3 Element contents related to sedimentary environment of coals in the Shanxi Formation (μg/g).

Sample	Co	U	Ni	Mo	Sr	Ba	Cu	B	Ga
ZJ-1	22.83	2.42	13.57	5.54	115.44	41.38	45.4	109.04	10.53
ZJ-2	10.28	3.04	6.39	3.52	185.54	89.64	9.88	167.34	13.72
ZJ-3	5.89	2.10	6.34	1.33	207.15	77.93	37.11	225.36	9.72
ZJ-4	6.50	0.83	9.46	1.71	299.92	117.68	20.04	164.13	6.87
ZJ-5	3.61	1.59	9.51	2.53	226.97	59.44	19.28	159.54	5.14
ZJ-6	3.40	1.13	8.33	3.26	543.59	55.94	42.52	200.70	4.14
ZJ-7	2.47	3.97	3.98	1.89	879.16	126.31	6.02	144.56	12.55
ZJ-8	1.79	5.25	6.74	1.36	281.10	136.76	23.2	168.49	14.54
ZJ-9	1.65	4.15	3.64	1.42	453.11	72.11	11.61	211.36	11.71
XJ-1	16.13	1.39	9.18	2.88	789.11	44.53	34.91	67.59	12.36
XJ-2	15.62		10.40	3.15	740.44	66.22	34.26	52.32	10.88
XJ-3	10.61	2.28	15.02	4.04	223.64	135.69	38.09	196.70	12.76
XJ-4	2.84	2.27	15.01	3.07	171.29	89.86	39.51	100.70	7.36
XJ-5	3.78	3.47	7.26	1.88	375.33	79.23	32.29	136.31	13.54
XJ-6	2.68	1.64	15.30	2.09	707.06	69.28	33.29	114.43	5.66
XJ-7	1.41	1.24	5.19	2.09	564.62	63.49	16.9	354.60	4.22
XJ-8	2.70	3.3	7.17	1.09	492.19	81.74	21.06	187.96	11.40
XJ-9	10.08	2.64	4.12	0.91	418.39	127.83	16.65	199.11	20.38
XJ-10	8.65	1.28	5.30	1.32	482.47	83.55	21.26	58.17	12.48
XJ-11	2.26	2.87	4.32	0.25	346.89	112.18	20.72	168.01	10.76
XJ-12	2.22	2.12	6.09	1.31	663.53	63.72	30.99	289.20	7.30
XJ-13	3.60	1.75	11.73	2.74	375.98	45.91	36.42	118.71	8.72
XJ-14	6.34	1.53	5.35	1.96	1742.71	83.62	14.14	180.93	9.14
XJ-15	5.33	1.28	3.96	0.80	401.83	42.01	13.65	155.50	10.69
XJ-16	2.62	1.47	3.38	1.18	304.84	72.00	5.85	131.31	4.22
XJ-17	3.50	2.07	4.32	1.80	245.82	72.30	11.18	149.96	5.79

affected by the water barrier island-tidal flat-lagoon wetland environment. The C value of Zhangji coal samples range from 0.14 to 1.68, with an average value of 0.50. In the vertical direction, only ZJ-2 and ZJ-7 to ZJ-8 were affected by land sources, and the study area as a whole was mainly affected by sea-land cross deposition. The C value of the coal samples from Xinjier mine range from 0.10 to 0.41, with an average value of 0.21. In the vertical direction, the upper coal seams were affected by seawater, while the and lower coal seams were affected by land sources, and ocean-land cross deposition mainly affected by land sources was formed on the whole (Figure 4).

4.2 Mercury distribution

4.2.1 Mercury content in coal seam

The mercury concentrations of Zhangji and Xinjier Mine are shown in Table 2. In order to evaluate of mercury content in coal seam, It also lists the average concentration of America coal, world coal, crust coals, as well as other region coals in China. The mercury content of coal in the study area ranges from 0.03 to 0.93 μg/g, and the arithmetic mean value is 0.21 μg/g, which is lower than the mean value of mercury in coal in Huaibei region and higher than that of North China coal, China coal, the world coal and other regions.

4.2.2 Distribution of mercury in coal seam

Although the coal samples of Zhangji and Xinjier mine are coal seams formed in the same period, the distribution of mercury content in coal is obviously different (Figure 5). The mercury content distribution in Zhangji coal samples show a downward trend in the vertical direction, but the overall enrichment degree is relatively stable. In the Xinjier coal seam, the minimum mercury content is only 0.03 μg/g and the maximum content is 0.93 μg/g, the difference up to 30 times. According to the variation of mercury content in vertical section, all samples were divided into two groups: group 1 (XJ-1–XJ-6) and group 2 (XJ-7–XJ-17). The mercury content of coal changes in the group 1 near the roof are similar to those

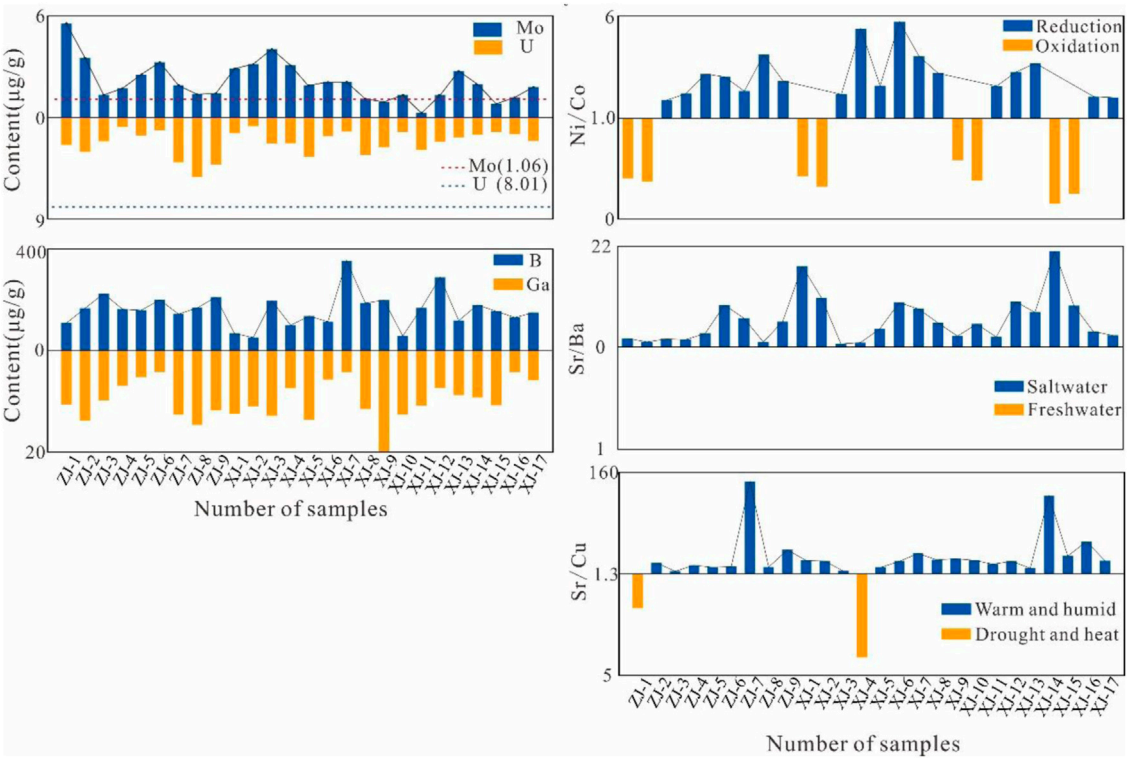

FIGURE 6
Characteristics of depositional environment.

in the Zhangji coal mine, the group two has very low mercury content in the coal near the floor, but the content changes are relatively stable. Compared with the mercury in the earth's crust, it appears dispersed. In many other studies it has been observed that some elements accumulations are prevalent in the floor, roof, or the coal samples near them. This means that host rocks (floor and roof) significantly carry these elements, and terrigenous inputs may primarily influence the distribution of these elements in coal seams. (Chen et al., 2011; Fu et al., 2016; Ding et al., 2018).

4.3 Origin of mercury

4.3.1 Characteristics of depositional environment

In this paper, the content distribution of mercury of coal seam are associated with the depositional environment characteristics, and the causes of mercury accumulation in coal are analyzed. The redox conditions in the depositional environment are usually characterized by the enrichment degree of U and Mo elements and the Ni/Co ratio (Kimura and Watanabe., 2001; Tribovillard et al., 2006; Wang X. et al., 2018). As shown in Table 3, the content of U in Zhangji Mine coal samples ranges from 0.83 to 5.25 μg/g (avg. 2.72 μg/g), and the content of Mo ranges from 1.33 to 5.54 μg/g (avg. 2.51 μg/g); The content of U in Xinjier Mine coal samples is 0.77–3.47 μg/g (avg. 1.96 μg/g), and the content of Mo is 0.25–4.04 μg/g (avg. 1.92 μg/g). Compared with U (8.10 μg/g) and Mo (1.06 μg/g) in The Upper crust of China, the two groups of coal samples show U deficit and Mo enrichment. The Ni/Co ratio of Zhangji Mine coal sample is between 0.59 and 3.77, and the Ni/Co ratio of Xinjier Mine coal samples is between 0.41 and 5.71 (avg. 3.49). According to the numerical results, the study area showed a transition from oxidizing environment to reducing environment, and which indicated a weak oxidation-reduction environment (Figure 6).

B, Ga and Sr/Ba ratio are indictors of the paleosalinity of the depositional environment. The content of B is high in seawater deposition, whereas the content of Ga is high in fresh water deposition (Dai et al., 2016; Wang et al., 2021). A previous study showed that Sr/Ba>1 indicates a marine depositional environment. On the contrary, it indicates a Continental depositional environment (Du et al., 2009; Chen et al., 2013). With the vertical cross section downward, both B and

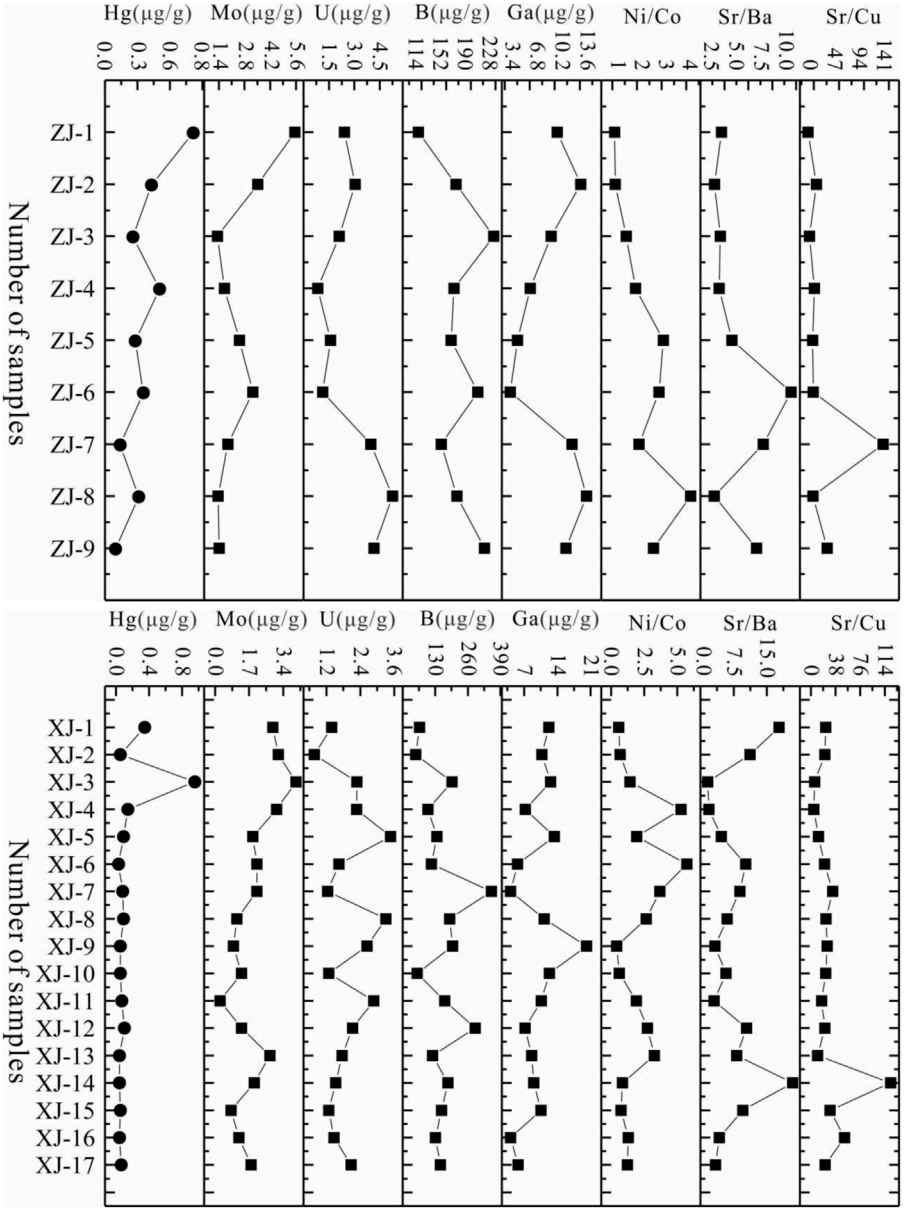

FIGURE 7
The characteristic content distribution of mercury and depositional environment in coal.

Ga have irregular changes, reflecting the alternating deposition of sea and land. With the change of formation thickness, the content of B in the study area shows a peak value in ZJ-3, ZJ-6, ZJ-9, XJ-3, XJ-7, and XJ-12, indicating that the location was severely affected by seawater. The Sr/Ba ratio of Zhangji Mine coal samples ranges from 2.06 to 9.72 (avg. 4.32). The Sr/Ba ratio of Xinjier Mine coal samples ranges from 1.65 to 20.84 (avg. 7.71), manifesting that the study area indicated the Marine salt water depositional environment (Table 3; Figure 6).

The ratio of Sr/Cu can be used as a sensitive indicator to reflect the change of climatic conditions. The Sr/Cu value is low (1.3<Sr/Cu>5.0), reflecting the warm and humid depositional environment. Otherwise, the Sr/Cu ratio is high value (Sr/Cu>5.0) reflects dry and hot climatic conditions (Liu et al., 2022). The Sr/Cu values of Zhangji Mine coal samples ranges from 2.54 to 146.04 (avg. 29.29). The Sr/Cu values of Xinjier Mine ranges from 4.34 to 123.25, (avg.27.48). Therefore, the climate indication of the study area was a transition from warm

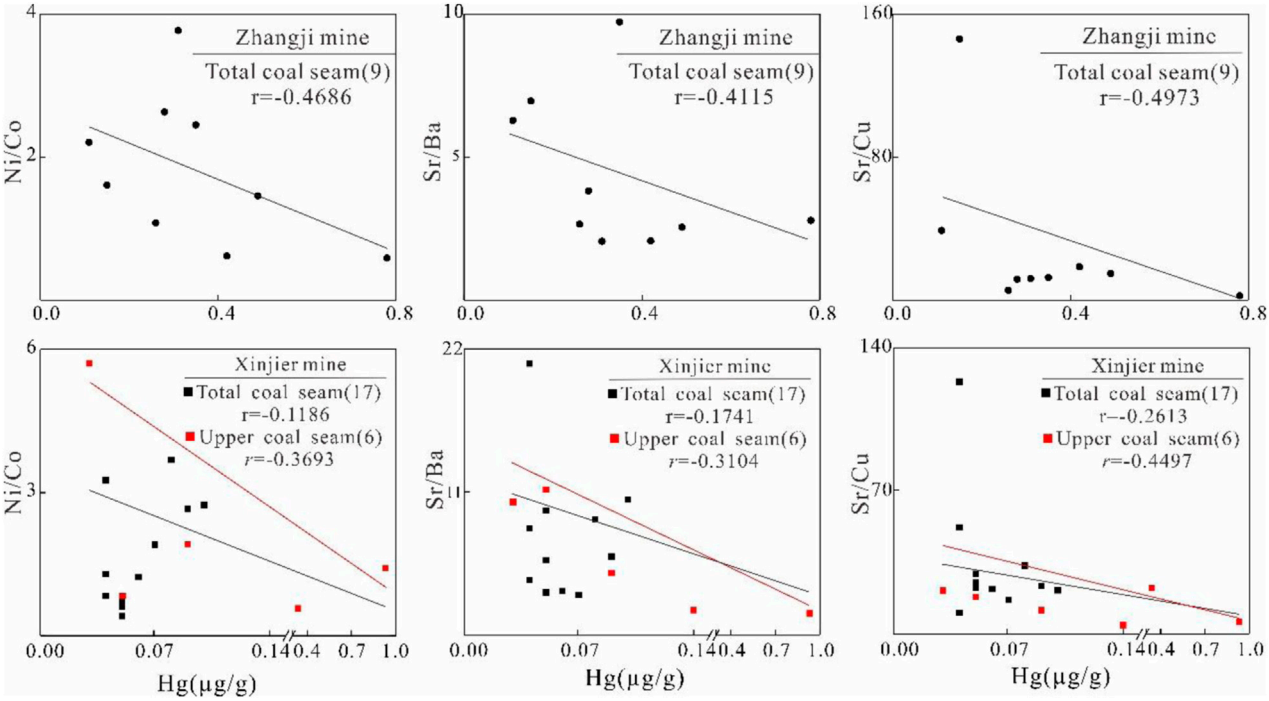

FIGURE 8
Correlation analysis of mercury and depositional environment in coal.

and humid to dry and hot in the process of coal formation (Table 3; Figure 6).

4.3.2 Relationship between redox conditions and mercury content distribution in coal

In the process of coal formation, redox conditions also play an important role in the transformation of plant remains into humus and in the precipitation complexation and precipitation of trace elements in humus (Nechaev et al., 2022; Shi et al., 2022). The mercury content in Zhangji mine coal samples is distributed on the vertical cross section, the change trend of Ni/Co ratio is opposite, and similar to that of Mo content, showing a trend of decrease and then increase (Figure 7). The correlation analysis showed that $r_{Hg\text{-}Ni/Co}$=−0.4686, indicating that mercury in coal is easy to accumulate in the oxidizing environment and to migrate in the reducing environment. The changes of mercury content in Group 1 in Xinjier Mine are similar to the Ni/Co ratio and Mo content. Group two have no obvious changes with the increase of vertical formation thickness. It can be seen from the correlation index, Overall coal seam $r_{Hg\text{-}Ni/Co}$=−0.1186, upper coal seam (Group 1) $r_{Hg\text{-}Ni/Co}$=−0.3693, indicating that mercury in coal is also easily enriched in an oxidizing environment, but redox conditions have a greater impact on mercury in upper coal seams, and have no effect on lower coal seams (Figure 8). Mercury of coal in the study area is easy to accumulate in the oxidized deposition environment, mainly because the oxidized environment was conducive to the decomposition and transformation of organic matter by microorganisms. In this process, mercury was easy to transform the soluble compound to form precipitation, leading to the reduction of migration ability and then enrichment (Zhu et al., 2021).

4.3.3 Relationship between paleosalinity conditions and mercury content distribution in coal

The salinity of the water medium in the coal-forming environment affects the dissolution, precipitation, complexation and adsorption of trace elements in the swamp (Sun et al., 2012; Oboirien et al., 2016). The mercury content of ZJ-1~ZJ-4 in Zhangji coal sample does not change obviously with the paleosalinity, but the mercury content of ZJ-5~ZJ-9 coal sample changes in reverse with the paleosalinity (Figure 7). The correlation index of $r_{Hg\text{-}Sr/Ba}$=−0.4115 indicates that the salt water conditions are not conducive to mercury enrichment. In the upper coal seam, mercury is the least affected by salt water; in the middle coal

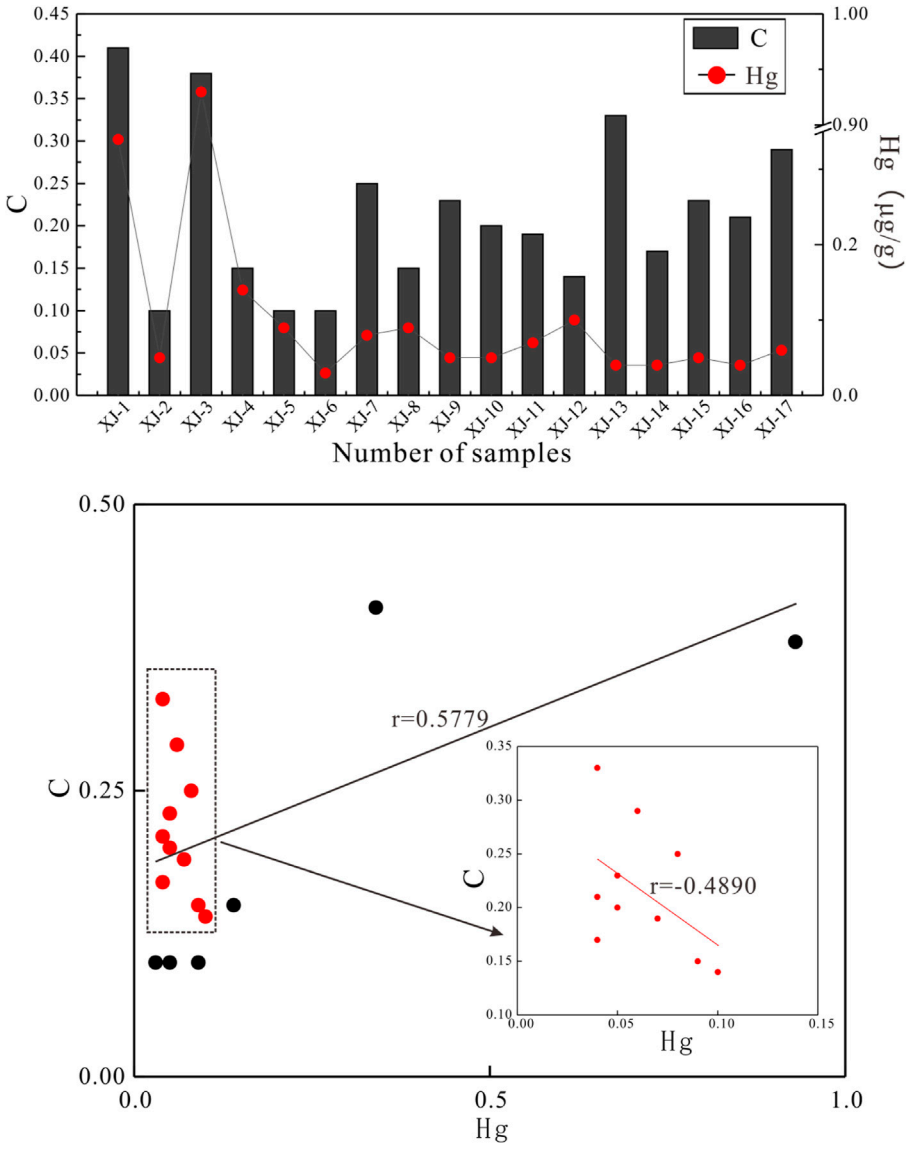

FIGURE 9
Correlation analysis of mercury and terrigenous inputs.

seam, it is the most affected by salt water; in the lower coal seam, the salinity of sea water shows a decreasing trend, and the content of mercury in coal increases slightly. The mercury content of Group one in Xinjier Mine coal decreases gradually with the change of paleosalinity, and has a peak value in XJ-3 coal sample. There is no obvious relationship between the change trend of mercury in Group one coal samples and paleosalinity. The correlation index shows that the overall coal seam $r_{Hg\text{-}Sr/Ba}$=−0.1741, and the upper coal seam (Group one) $r_{Hg\text{-}Sr/Ba}$=−0.3104, indicating that the upper coal seam is strongly affected by saline water environment, while the lower coal seam is affected by other geological activities The effect of salinity is greater than that of water (Figure 8). In this sense, we conclude that the freshwater-dominated environment was likely to be more conducive to mercury accumulation than the marine-dominated environment, which was consistent with the previous research results (Wang G. et al., 2018).

4.3.4 Relationship between palaeoclimate conditions and mercury content in coal

Climate change during coal formation is an important primary factor for the migration and enrichment of trace

elements in coal (Milleson et al., 2016). The mercury content of ZJ-1~ZJ-3 and ZJ-6~ZJ-9 in Zhangji Mine coal sample shows an obvious opposite trend with the change of Sr/Cu ratio. According to the correlation index $r_{Hg\text{-}Sr/Cu}$=−0.4973, indicating that hot and dry climate is not conducive to the accumulation of mercury in Zhangji coal. The mercury content in Group 1 coal samples of Xinjier Mine coal samples shows an opposite trend with the change of climatic conditions, and peaked at XJ-3. The mercury content in Group two coal samples is not closely related to climate change (Figure 7). According to the correlation index, $r_{Hg\text{-}Sr/Cu}$=−0.2613 on the whole and $r_{Hg\text{-}Sr/Cu}$=−0.4497 on the upper coal seam, indicating that the upper coal seam is strongly affected by climate while the lower coal seam is weakly affected by climate, which may be disturbed by other geological factors. Therefore, the study showed that compared with the hot and dry climate, the warm and humid depositional environment was more conducive to the accumulation of mercury in coal in the study area (Lv et al., 2020). The dry coal-forming environment may affect the species, flourishing degree of organic organisms and decomposition rate of plant remains, thus affecting the migration and enrichment of harmful trace elements in swamp organisms (Lu et al., 2020) (Figure 8).

4.3.5 Influence of terrigenous inputs

The mechanical transport of minerals will be caused by the input of continental clasts in coal seams, which will lead to the migration and enrichment of trace elements in coal carried by a large number of mineral clasts (Wang et al., 2022a; Wang et al., 2022b). The upper coal seam of Xinjier Mine is affected by redox, paleosalinity and paleoclimate in the depositional environment, and the lower coal seam is affected by various geological activities. The depositional facies of the study area is the ocean-land cross deposition dominated by terrigenous inputs, and the lower coal seam is strongly influenced by terrigenous inputs. As shown in Figure 9, the variation trend of C value in Xinjier Mine indicates that the depositional environment is gradually transferred from seawater activity to terrigenous inputs, mercury content of Group one (XJ-1~ XJ-6) showes an increasing trend with seawater activity, while mercury content of Group two (XJ-7-XJ-17) showes a decreasing trend with the intensification of terrigenous inputs. Through correlation analysis, it is found that $r_{Hg\text{-}C}$=0.5779 on the whole coal seam and $r_{Hg\text{-}C}$=−0.4890 on the lower coal seam. The results showed that the terrigenous input in the sedimentary environment is not conducive to the accumulation of mercury in coal.

5 Conclusion

The mercury content in coal of Shanxi Formation in the deep part of the study area ranged from 0.03 to 0.93 μg/g, and the mean value was 0.21 μg/g, which was higher than the background value of mercury in coal of China (0.19 μg/g) and the world (0.1 μg/g). Compared to the content of mercury in the Crust (0.08 μg/g), the enrichment coefficient was 2.6, which showed significant enrichment. Kaolinite, quartz and pyrite are the main minerals in the coal in the study area. The distribution of mercury content in shanxi formation coal in the deep part of Huainan coalfield is very different due to depositional environment. The content of mercury in the coal of Shanxi Formation of Zhangji Coal Mine ranges from 0.11 to 0.78 μg/g, with the mean value of 0.35 μg/g. The content of mercury in coal of Shanxi Formation of Xinjier mine coal ranges from 0.03 to 0.93 μg/g, with the mean value of 0.12 μg/g.

The sedimentary rocks of the Shanxi Formation belong to the middle-acid bedrock, and the depositional facies are represented by sea-land alternate facies. The climatic conditions are mainly composed of warm and humid to arid and hot transitional sedimentary environment. The enrichment of mercury in coal in Zhangji mining area is mainly affected by the redox conditions, paleosalinity and paleoclimate in the depositional environment. The upper coal seam of mercury in Xinjier coal mine is affected by various geological factors in depositional environment: the upper coal seam is affected by redox conditions, paleosalinity and paleoclimate in depositional environment; The lower coal seam is affected by land source input. The results show that land source input is not conducive to mercury enrichment and sea water activity is conducive to the enrichment of mercury in a certain extent.

Data availability statement

The original contributions presented in the study are included in the article/supplementary material, further inquiries can be directed to the corresponding author.

Author contributions

LGZ: Writing—review and editing, Conceptualization, Resources, Funding acquisition, and Supervision. LQZ: Data collection, Data analyzing, Methodology, Software, Writing—original draft. (LQZ is the co-first author, consistent with LGZ's contribution). YW, YYC: Data curation, Validation, Investigation. YCC: Resources. SA, YX: Writing—review and editing. All authors provided critical feedback and helped shape the research analysis and manuscript.

Funding

This research was supported by the National Natural Science Foundation of China (42072201) and the University Synergy Innovation Program of Anhui Province (GXXT-2021-017).

Conflict of interest

The authors declare that the research was conducted in the absence of any commercial or financial relationships that could be construed as a potential conflict of interest.

The reviewer JC declared a shared affiliation with the authors YCC, SA, and YX to the handling editor at the time of review.

Publisher's note

All claims expressed in this article are solely those of the authors and do not necessarily represent those of their affiliated organizations, or those of the publisher, the editors and the reviewers. Any product that may be evaluated in this article, or claim that may be made by its manufacturer, is not guaranteed or endorsed by the publisher.

References

Chen, B., Liu, G., and Sun, R. (2016). Distribution and fate of mercury in pulverized bituminous coal-fired power plants in coal energy-dominant huainan city, China. *Arch. Environ. Contam. Toxicol.* 70, 724–733. doi:10.1007/s00244-016-0267-7

Chen, H., Liu, K., Shi, T., and Wang, L. (2022). Coal consumption and economic growth: A Chinese city-level study. *Energy Econ.* 109, 105940. doi:10.1016/j.eneco.2022.105940

Chen, J., Liu, G, J., Kang, Y., Wu, B., Sun, R., Zhou, C., et al. (2013). Atmospheric emissions of F, As, Se, Hg, and Sb from coal-fired power and heat generation in China. *Chemosphere* 90, 1925–1932. doi:10.1016/j.chemosphere.2012.10.032

Chen, J., Liu, G, J., Kang, Y., Wu, B., Sun, R., Zhou, C., et al. (2014a). Coal utilization in China: Environmental impacts and human health. *Environ. Geochem. Health* 36, 735–753. doi:10.1007/s10653-013-9592-1

Chen, J., Liu, G, J., Li, H., and Wu, B. (2014b). Mineralogical and geochemical responses of coal to igneous intrusion in the Pansan coal mine of the Huainan coalfield, Anhui, China. *Int. J. Coal Geol.* 124, 11–35. doi:10.1016/j.coal.2013.12.018

Cheng, M. M., Zhi, G. R., Tang, W., Liu, S. J., Dang, H. Y., Guo, Z., et al. (2017). Air pollutant emission from the underestimated households' coal consumption source in China. *Sci. Total Environ.* 580, 641–650. doi:10.1016/j.scitotenv.2016.12.143

Chen, J., Liu, G., Jiang, M., Chou, C. L., Li, H., Wu, B., et al. (2011). Geochemistry of environmentally sensitive trace elements in Permian coals from the Huainan coalfield, Anhui, China. *Int. J. Coal Geol.* 88, 41–54. doi:10.1016/j.coal.2011.08.002

Chen, X., Zheng, L., Jiang, Y., and Jiang, C. (2021). Transformation of minerals at the boundary of magma-coal contact zone: Case study from wolonghu coal mine, Huaibei coalfield, China. *Int. J. Coal Sci. Technol.* 8 (1), 168–175. doi:10.1007/s40789-020-00373-6

Chou, C, L. (2012). Sulfur in coals: A review of geochemistry and origins. *Int. J. Coal Geol.* 100, 1–13. doi:10.1016/j.coal.2012.05.009

Dai, S, F., Han, D, X., and Chou, C, L. (2006). Petrography and geochemistry of the middle devonian coal from luquan, yunnan province, China. *Fuel* 85, 456–464. doi:10.1016/j.fuel.2005.08.017

Dai, S, F., Liu, J, J., Ward, C, R., Hower, J. C., French, D., Jia, S., et al. (2016). Mineralogical and geochemical compositions of Late Permian coals and host rocks from the Guxu Coalfield, Sichuan Province, China, with emphasis on enrichment of rare metals. *Int. J. Coal Geol.* 166, 71–95. doi:10.1016/j.coal.2015.12.004

Dai, S, F., Ren, D, Y., Chou, C-L., Finkelman, R. B., Seredin, V. V., and Zhou, Y. (2012). Geochemistry of trace elements in Chinese coals: A review of abundances, genetic types, impacts on human health, and industrial utilization. *Int. J. Coal Geol.* 94, 3–21. doi:10.1016/j.coal.2011.02.003

Dai, S, F., Zhang, W., Ward, C, R., Seredin, V. V., Hower, J. C., Li, X., et al. (2013). Mineralogical and geochemical anomalies of late permian coals from the fusui coalfield, guangxi province, southern China: Influences of terrigenous materials and hydrothermal fluids. *Int. J. Coal Geol.* 105, 60–84. doi:10.1016/j.coal.2012.12.003

Ding, D, S., Liu, G, J., Fu, B., and Cuicui, Q. (2018). Characteristics of the coal quality and elemental geochemistry in Permian coals from the Xinjier mine in the Huainan Coalfield, north China: Influence of terrigenous inputs. *J. Geochem. Explor.* 186, 50–60. doi:10.1016/j.gexplo.2017.12.002

Du, G., Zhuang, X, M., Querol, X., Izquierdo, M., Alastuey, A., Moreno, T., et al. (2009). Gedistribution in the Wulantuga high-germanium coal deposit in the Shengli coalfield, Inner Mongolia, northeastern China. *Int. J. Coal Geol.* 78, 16–26. doi:10.1016/j.coal.2008.10.004

Eskenazy, G., Finkelman, R, B., and Chattarjee, S. (2010). Some considerations concerning the use of correlation coefficients and cluster analysis in interpreting coal geochemistry data. *Int. J. Coal Geol.* 83, 491–493. doi:10.1016/j.coal.2010.05.006

Finkelman, R, B. (1993). *Trace and minor elements in coal Organic Geochemistry*, 28. New York: Plenum, 593–607.

Fu, B., Liu, G., Liu, Y., Cheng, S., Qi, C., and Sun, R. (2016). Coal quality characterization and its relationship with geological process of the Early Permian Huainan coal deposits, southern North China. *J. Geochem. Explor.* 166, 33–44. doi:10.1016/j.gexplo.2016.04.002

Guo, S., Zhang, L., Niu, X., Gao, L., Cao, Y., Wei, X. X., et al. (2018). Mercury release characteristics during pyrolysis of eight bituminous coals. *Fuel* 222, 250–257. doi:10.1016/j.fuel.2018.02.134

Harrar, H., Eterigho, O., Modiga, A., and Bada, S. (2022). Mineralogy and distribution of rare Earth elements in the Waterberg coalfield high ash coals. *Min. Eng.* 183, 107611. doi:10.1016/j.mineng.2022.107611

Hu, Y, N., and Cheng, H, F. (2016). Control of mercury emissions from stationary coal combustion sources in China: Current status and recommendations. *Environ. Pollut.* 218, 1209–1221. doi:10.1016/j.envpol.2016.08.077

Kimura, H., and Watanabe, Y. (2001). Oceanic anoxia at the Precambrian-Cambrian boundary. *Geol.* 29, 995–998. doi:10.1130/0091-7613(2001)029<0995:oaatpc>2.0.co;2

Li, C. H., Liang, H, D., Wang, S, K., and Liu, J. (2018). Study of harmful trace elements and rare Earth elements in the Permian tectonically deformed coals from Lugou mine, North China Coal Basin, China. *J. Geochem. Explor.* 190, 10–25. doi:10.1016/j.gexplo.2018.02.016

Liu, D., Fan, Q., Zhang, C., Gao, Y., Du, W., Song, Y., et al. (2022). Paleoenvironment evolution of the permian lucaogou Formation in the southern junggar basin, NW China. *Palaeogeogr. Palaeoclimatol. Palaeoecol.* 603, 111198. doi:10.1016/j.palaeo.2022.111198

Lu, J., Zhou, K., Yang, M., Eley, Y., Shao, L., and Hilton, J. (2020). Terrestrial organic carbon isotopic composition (δ13Corg) and environmental perturbations linked to Early Jurassic volcanism: Evidence from the Qinghai-Tibet Plateau of China. *Glob. Planet. Change* 195, 103331. doi:10.1016/j.gloplacha.2020.103331

Luo, G., Ma, J., Han, J., Yao, H., Xu, M., Zhang, C., et al. (2013). Hg occurrence in coal and its removal before coal utilization. *Fuel* 104, 70–76. doi:10.1016/j.fuel.2010.04.004

Lv, D., Li, Z., Wang, D., Li, Y., Liu, H., Liu, Y., et al. (2019). Sedimentary model of coal and shale in the Paleogene Lijiaya Formation of the Huangxian Basin: insight from petrological and geochemical characteristics of coal and shale. *Energy Fuels* 33 (11), 10442–10456. doi:10.1021/acs.energyfuels.9b01299

Lv, D., Song, Y., Shi, L., Wang, Z., Cong, P., and van Loon, A. T. (2020). The complex transgression and regression history of the northern margin of the Palaeogene Tarim Sea (NW China), and implications for potential hydrocarbon occurrences. *Mar. Petrol Geol.* 112, 104041. doi:10.1016/j.marpetgeo.2019.104041

Milleson, M., Myers, T., and Tabor, N. (2016). Permo-carboniferous paleoclimate of the Congo Basin: Evidence from lithostratigraphy, clay mineralogy, and stable isotope geochemistry. *Palaeogeogr. Palaeoclimatol. Palaeoecol.* 441 (2), 226–240. doi:10.1016/j.palaeo.2015.09.039

Nechaev, V., Dai, S., Chekryzhov, I., Tarasenko, I. A., Zin'kov, A. V., and Moore, T. A. (2022). Origin of the tuff parting and associated enrichments of Zr, REY, redox-sensitive and other elements in the Early Miocene coal of the Siniy Utyes Basin, southwestern Primorye, Russia. *Int. J. Coal Geol.* 250, 103913. doi:10.1016/j.coal.2021.103913

Oboirien, B, O., Thulari, V., and North, B, C. (2016). Enrichment of trace elements in bottom ash from coal oxy-combustion: Effect of coal types. *Appl. Energy* 177, 81–86. doi:10.1016/j.apenergy.2016.04.118

Qin, S., Gao, K., Sun, Y., Wang, J., Zhao, C., Li, S., et al. (2018). Geochemical characteristics of rare-metal, rare-scattered, and rare-Earth elements and minerals in the Late Permian coals from the Moxinpo mine, Chongqing, China. *Energy fuels.* 32, 3138–3151. doi:10.1021/acs.energyfuels.7b03791

Shi, Q., Li, C., Wang, S., Li, D., Wang, S., Du, F., et al. (2022). Effect of the depositional environment on the Formation of tar-rich coal: A case study in the northeastern ordos basin, China. *J. Pet. Sci. Eng.* 216, 110828. doi:10.1016/j.petrol.2022.110828

Sun, Y, Z., Zhao, C, L., Li, Y, H., Wang, J., and Liu, S. (2012). Li distribution and mode of occurrences in Li-bearing coal seam # 6 from the Guanbanwusu Mine, Inner Mongolia, Northern China. *Energy Explor. Exploitation* 30, 109–130. doi:10.1260/0144-5987.30.1.109

Tian, H, Z., Liu, K, Y., Zhou, J, R., Lu, L., Hao, J., Qiu, P., et al. (2014). Atmospheric emission inventory of hazardous trace elements from China's coal-fired power plants temporal trends and spatial variation characteristics. *Environ. Sci. Technol.* 48, 3575–3582. doi:10.1021/es404730j

Tribovillard, N., Algeo, T, J., Lyons, T., and Riboulleau, A. (2006). Trace metals as paleoredox and paleoproductivity proxies: An update. *Chem. Geol.* 23, 12–32. doi:10.1016/j.chemgeo.2006.02.012

United Nations Environment Programme (2019). *Global mercury assessment 2018*. Geneva: Chemicals and Health Branch.

Wang, A., Wang, Z., Liu, J., Xu, N., and Li, H. (2021). The Sr/Ba ratio response to salinity in clastic sediments of the Yangtze River Delta. *Chem. Geol.* 559, 119923. doi:10.1016/j.chemgeo.2020.119923

Wang, E., Guo, T., Li, M., Li, C., Dong, X., Zhang, N., et al. (2022a). Exploration potential of different lithofacies of deep marine shale gas systems: Insight into organic matter accumulation and pore formation mechanisms. *J. Nat. Gas. Sci. Eng.* 102, 104563. doi:10.1016/j.jngse.2022.104563

Wang, L., Lv, D., Hower, J. C., Zhang, Z., Raji, M., Tang, J., et al. (2022b). Geochemical characteristics and paleoclimate implication of Middle Jurassic coal in the Ordos Basin, China. *Ore. Geol. Rev.* 144, 104848.

Wang, G., Xie, Y, W., Qin, Y., Wang, J., Shen, J., Han, B., et al. (2018). Element geochemical characteristics and formation environment for the roof, floor and gangue of coal seams in the Gujiao mining area, Xishan coalfield, China. *J. Geochem. Explor.* 190, 336–344. doi:10.1016/j.gexplo.2018.04.007

Wang, X., Wu, D., Liu, G., and Sun, R. (2018). Variation of Hg content in low sulfur coals in relation to the coal-forming environment: A case study from Zhuji coal mine, huainan coalfield, north China. *Environ. Earth Sci.* 77 (19), 703. doi:10.1007/s12665-018-7861-0

Wei, Q., Hu, B., Li, X., Feng, S., Xu, H., Zheng, K., et al. (2021). Implications of geological conditions on gas content and geochemistry of deep coalbed methane reservoirs from the Panji Deep Area in the Huainan Coalfield, China. *J. Nat. Gas Sci. Eng.* 85, 103712. doi:10.1016/j.jngse.2020.103712

Yang, Y., Liu, J., and Wang, Z. (2020). Reaction mechanisms and chemical kinetics of mercury transformation during coal combustion. *Prog. Energy Combust. Sci.* 79, 100844. doi:10.1016/j.pecs.2020.100844

Zhang, B., Chen, J., Sha, J., Zhang, S., Zeng, J., Chen, P., et al. (2020). Geochemistry of coal thermally-altered by igneous intrusion: A case study from the pansan coal mine of huainan coalfield, Anhui, eastern China. *J. Geochem. Explor.* 213, 106532. doi:10.1016/j.gexplo.2020.106532

Zhang, J, Y., Ren, D, Y., and Xu, D, W. (1999). *Distribution of arsenic and mercury in triassic coals from longtoushan syncline, southsestern guizhou*. Guizhou: Shanxi Science Technology Press. Prospects for Coal Science in 21st Century, 153–156.

Zhang, L, Q., Zheng, L, G., and Liu, M. (2022). Study on the mineralogical and geochemical characteristics of arsenic in permian coals: Focusing on the coalfields of shanxi formation in northern China. *Energies* 15 (9), 3185. doi:10.3390/en15093185

Zhang, Q., Zheng, L., Han, B., Zhang, J., Cai, Y. J., and Xing, D. W. (2022). Mineralogical characteristics of the shanxi formation coal in the huainan coalfield, Anhui, China. *Bull. Mineralogy, Petrology Geochem.* 41 (03). (in Chinese). doi:10.19658/j.issn.10072802.2022.41.006

Zhao, S., Pudasainee, D., Duan, Y., Gupta, R., Liu, M., and Lu, J. (2019). A review on mercury in coal combustion process: Content and occurrence forms in coal, transformation, sampling methods, emission and control technologies. *Prog. Energy Combust. Sci.* 73, 26–64. doi:10.1016/j.pecs.2019.02.001

Zheng, L. G., Liu, G. J., and Qi, C. C. (2007a). Environmental geochemistry of mercury in coal in China. *J. Univ. Sci. Technol. China* 37, 953–963. (in Chinese).

Zheng, L. G., Liu, G. J., and Qi, C. C. (2007b). Occurrence of mercury in coal of Huaibei coalfield. *Earth Science-Journal China Univ. Geosciences* 32, 279–284. (in Chinese).

Zhu, G., Wang, P., Li, T., Zhao, K., Yan, H., Li, J., et al. (2021). Nitrogen geochemistry and abnormal mercury enrichment of shales from the lowermost Cambrian Niutitang Formation in South China: Implications for the marine redox conditions and hydrothermal activity. *Glob. Planet. Change* 199, 103449. doi:10.1016/j.gloplacha.2021.103449